THERMAL AND KINEMATIC ATTRIBUTES OF UPWIND DIRECTED JETS

M. Moeller[1]
Department of Mechanical Engineering
Michigan State University
East Lansing, MI 48824

P. Solfrank[1], **A.F. Cawood**[2] **and J. F. Foss**[3]
Department of Mechanical Engineering
Michigan State University
East Lansing, MI 48824
foss@egr.msu.edu

ABSTRACT

The kinematic and the diffusive properties of an up-wind directed jet have been identified by a thermal marking technique. Sixty-six fast response thermocouples, placed in the plane of the jet exit, were used to record instantaneous planes of T(x=0, y, z) for two velocity ratios: Vj/U=2.3 and 1.3. In agreement with the observations from T.U. Berlin, these ratios represent relatively unstable (2.3) and relatively stable (1.3) kinematic fields.

INTRODUCTION

The flow from a circular tube (of diameter d and velocity V_j) which is initially parallel to and in the opposite direction from a uniform oncoming stream of velocity U, is termed an upwind directed jet. The laboratory version of this flow can serve as a model for various technological flows including reverse thrust propulsors and rapid mixing nozzles for combustors. The majority of the prior studies have been concerned with the stochastic properties of this generic flow field. Principal among these is the penetration distance (x_p) of the jet into the oncoming stream as documented, for example by Peck (1981), Morgan, et al. (1976) and Arendt, et al. (1956). A correlation: $x_p/D=f(V_j/U)$, is provided by these authors.

König and Fiedler (1991) established the jet-to-approach velocity ratio ($\alpha=V_j/U$)≈1.4 as the transition from a nominally axisymmetric flow field to one with substantial time dependencies. Yoda and Fiedler (1996) confirmed the earlier observations using planar laser induced fluorescence (LIF) with α values of 1.3…10. Their results play an important role in the interpretation of the present observations. Further studies by the T.U. Berlin researchers: Bernero and Fiedler (2000) made use of PIV on the jet axis centerline for α=1.3 and higher values. Their data were analyzed using POD methods.

The unique attribute of recovering information on the instantaneously defined thermal field for a plane in the flow field makes the present study somewhat different from these prior investigations. Specifically, the jet fluid was thermally marked and 66 fast response thermocouples were placed in the jet exit plane; see Fig. 1. The side view of Fig. 1a identifies the physical components of the experiment. The elongated and relatively large diameter cylinder serves as the heated plenum for the jet flow that is delivered (RHS) into the uniform and low disturbance level: $\tilde{u}/U \lesssim 0.5\%$, approach flow. Fig. 1b identifies the locations: +, of the 66 thermocouples with respect to the jet-tube (centered at y=z=0). The trace from z/D=–2.7 to z/D≳6 is later used to show time resolved temperature values in this x=0 plane.

Since the thermocouple outputs can be simultaneously sampled and stored, the primitive experimental data can be processed to demonstrate the kinematic as well as the diffusive properties of the upwind directed jet flow field.

The data presented in this communication were obtained by M. Moeller (1987) and documented in his 1987 Diplomarbeit.[4] The Moeller (1987) effort made effective use of the prior work by Solfrank (1985) on the up-wind directed jet and the experimental techniques that were developed by Wark and Foss (1988). It will be apparent, in the following descriptions, that the 1980's technology made the experimental program somewhat more difficult than it would have been with current technology. However, the basic physics of the subject flow are quite adequately revealed by these planes of elevated temperature. It is suggested that these data could serve as an excellent test case for a large eddy simulation (LES).

The processed experimental data provide, therefore, T(0,y,z,t) at the locations shown (Fig. 1) and for the discrete times t_j. These temperature values were further processed to reveal the diffusive and kinematic properties of the flow. The low disturbance and effectively unbounded ($\pm y_{max}/D \simeq 25$, and $\pm z_{max} \geq \pm y_{max}$) approach flow interacts with the jet fluid to: i) sweep it in the return flow direction past the plane of the

[1] Exchange student from the RWTH-Aachen, AIA, Prof. E. Krause
[2] Graduate research assistant
[3] Professor
[4] An Electronic copy of his thesis is available at http://www.egr.msu.edu/tsfl/TSFL%20Publications.htm

thermocouples, and ii) to reduce the peak temperatures by molecular diffusion of the thermal energy.

The following text presents a brief description of the physical experiment. The further sections present the results from the temperature {T(t)} measurements; concluding with a summary of the paper's content.

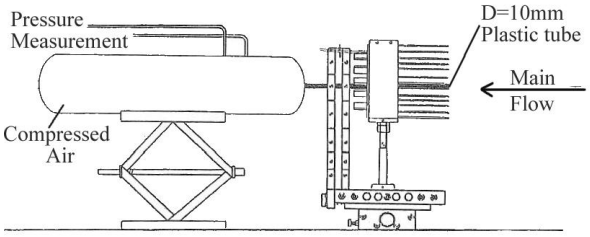

Fig 1a Jet Delivery System and Thermocouple Array

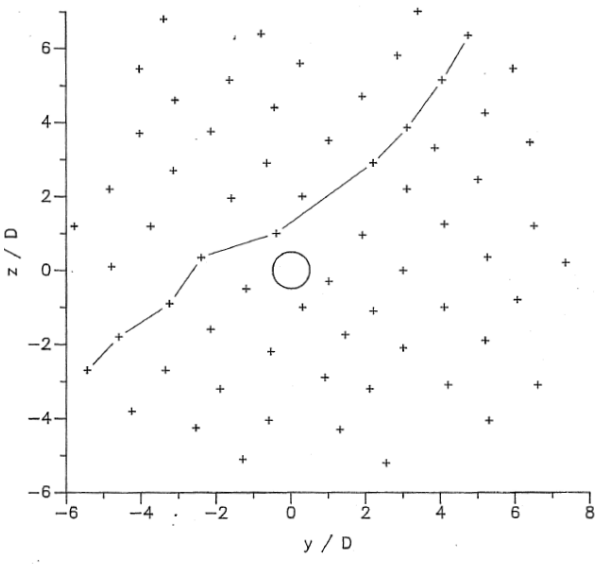

Fig 1b Location of the Thermocouples

Fig 1 Physical components of the experiment and the locations of the 66 thermocouples

THE FLOW SYSTEM

The length scale for this investigation is established by the 10mm ID plastic tube shown in Fig. 1a. The approach flow: ±250mm in y and ±400mm in z was uniform with a free stream velocity (U) of 2 m/sec and a disturbance level below 0.5%. Two different jet velocity magnitudes (V_j) were used: U=4.65 and 2.6m/sec.

The cylindrical chamber of Fig. 1a received de-oiled compressed air inside the steel pipe. The indicated outer diameter represents the insulation that covers the ohmic heating wires. The elevated jet-exit temperatures were provided by the I^2R power dissipation. The pressure measurement leads connect to static pressure taps that straddled an orifice plate. A flow meter was used to calibrate the orifice plate and a temperature sensor in the orifice outflow was used to determine the local density. Hence, the jet-exit spatially averaged velocity (V_j) could be determined from the known mass flow. Given the jet fluid temperature drop in the delivery tube, a thermocouple at the jet exit was used to obtain T(x=0, r=0).

Exit plane velocity and temperature surveys were carried out for the operating conditions such that the one-dimensional estimates could be corrected to the true flux values. The correction coefficients were satisfactorily close to unity: 0.957 for U=4.65m/sec. and 0.930 for U=2.6m/sec.

Temperature Field Measurements

Chromel-constantan, 5μm dia butt weld thermocouples were used to determine T(t) at the indicated locations of Fig. 1b. Their reference junctions were located near the processing electronics which consisted of four separate boards whose offset and ca 400× gain amplifiers delivered the signals to the four input ports of a 0-5v, 12-bit A/D converter. The processed signals were simultaneously sampled and held and delivered, via multiplexers, to the laboratory PDP 11-23 computer. The techniques to control and record the offset and gains and to provide post-acquisition filtering to remove the superimposed 60hz noise are detailed in Wark and Foss (1988).

The thermocouples can be reliably modeled as a first order dynamic system. Hence, their indicated (or bead) temperature (T_b), with respect to the true or fluid temperature (T_f) can be written as

$$T_f = T_b + \lambda \frac{dT_b}{dt} \quad \text{for } \lambda = m_b c / h A_b, \tag{1}$$

and the bead properties: m_b=mass, c=specific heat, A_b=area. Note that h=heat transfer coefficient. The value of h is, of course, a function of the Reynolds number.

Two forms of data were acquired. Low rate data, which were used to define the stochastic properties of the temperature field, were acquired with δt between samples equal to 40.96ms. Given the memory limitations of the PDP 11-73 microcomputer, the associated total sample time was τ_s=50.2sec. This sample period (τ_s) can be expressed in terms of the characteristic time scale as $\tau_s U/D=10^4$. Complementary data, acquired at the maximum rate of δt=0.64ms were corrected per equation 1 and these results are used to define the time resolved thermal and kinematic attributes of the upwind directed jets. The corresponding non-dimensional time between samples was Uδt/D=0.128.

Since the velocity at the thermocouple and at the time of measurement was not available, the λ values were determined for a characteristic flow speed (7 mps) and used with (1) to correct the high data rate $T_b(t)$ measurements (see Moeller (1987)). Note that a velocity correction was used to convert the 7 mps λ values to the λ values which were appropriate for the approach speed in this experiment; viz., U=2 m/sec. (The

higher velocity values (7 vs. 2 m/sec) led to a better definition of λ).

RESULTS AND DISCUSSION

Representative Time Series T(x=0, y_k/D, z_k/D)

Fig. 2 presents

$$T^* = \frac{[T(y_{i/D}, z_{k/D}, tU/D) - T_\infty]}{(T_j - T_\infty)} \qquad (2)$$

for the locations that were linked by the reference line in Fig. 1b for the V_j/U=2.3 condition. These values are immediately instructive regarding the essential data that are available in this investigation. Specifically:

i) The peak values are of order 0.2. This is a significant reduction from the jet-exit condition of 1.0 and it directly represents the cumulative effect of thermal diffusion since a given fluid dynamic particle can only lose or gain thermal energy by conduction[5] in the absence of radiation effects (radiation is negligible in this experiment).

ii) The locations that are "distant" from the jet-exit show intermittent patches of heated fluid. The intervening periods show the "flat" bottom $T=T_{ambient}$ traces given that ambient fluid occupies the thermocouple location during these periods.

iii) Locations near the jet-exit indicate continuously elevated temperatures albeit with substantial fluctuation levels.

Instantaneous Temperature Fields

With reference to Fig. 2, consider that a scan through all of the temperature values (not just those along the trace line of Fig. 1) at a given time was made. A contour plot of T*=constant magnitudes could be established at that given time. Viewing a series of these images would provide a graphical representation of the time dependant bent backwards jet column. A small sample of the Moeller (1987) images is presented in Figs. 3 and 4. Note that the circular jet opening (at 0,0) on these figures gives the reference location for the thermally active patches.

The noteworthy aspects of these images are: i) the thermal fields are relatively compact albeit certainly larger than the jet-exit area of their origin, and ii) the peak T* values mimic the Fig. 2 values where the magnitudes are of order. 0.2 for V_j/U=2.3. In contrast, the peak values are nominally 0.3 for V_j/U=1.3.

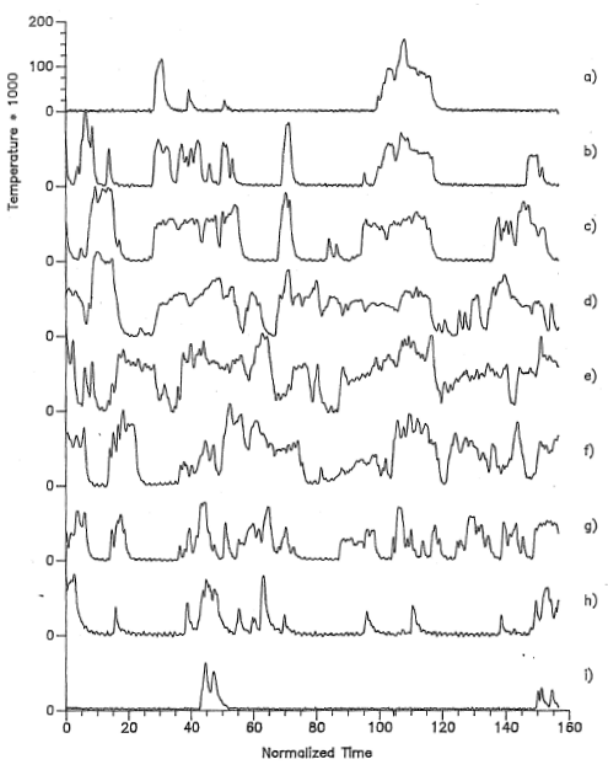

a) y/0=4.75, z/0=6.35 b) y/0=4.05, z/0=5.15
c) y /0=3.1, z/0=3.85 d) y /0=2.2, z/0=2.9
e) y/0=-0.4, z/0=1.0 f) y/0=-2.4, z/0=0.35
g) y/0=-3.25, z/0=-0.9 h) y/0=-4.6, z/0=-1.8
i) y/0=-5.45, z/0=-2.7

Fig. 2 Simultaneously sampled temperature at the locations along the trace-line of Fig 1b. V_J/U=2.3

Stochastic Values of Instantaneous Values

In characteristic Reynolds averaging fashion, the data at all of the discrete locations can be subject to the extraction of first and second moments. The results, for both velocity ratios and for the time mean values are presented in Figs. 5 and 6. Similarly, but with less smoothing, the standard deviation contours are provided by Moeller (1987), see his figures 37 and 38.

The T*=constant contours for the time averaged values can be compared with the instantaneous contours of the previous section. An immediate observation is the qualitative dissimilarity between the instantaneous and time averaged fields. The latter shows the expected (quasi) axisymmetry albeit the centroid is displaced from the origin. (Alignment plus buoyancy are considered to be responsible for this displacement). Concurrently the peak temperatures for the time mean values are substantially less than the instantaneous peaks. The more compact, lower velocity ratio case (V_j/U=1.3) shows a relatively larger peak temperature = 0.130 cf. 0.080.

[5] The thermal energy equation for a fluid dynamic particle in this experiment is $DT/Dt=\alpha\nabla^2T$ where $\alpha=k/\rho c_p$.

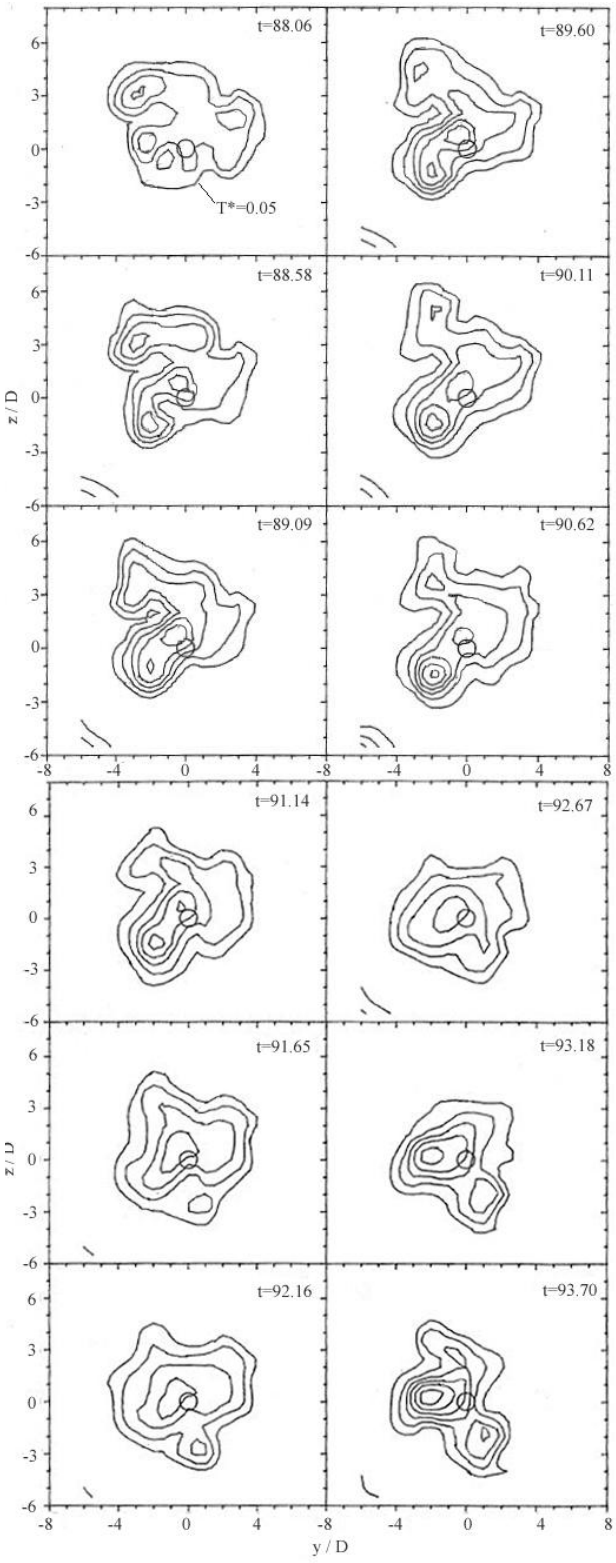

Fig. 3 Instantaneous Contours of Normalized Temperature, $V_J/U=1.3$ (First isotherm at T*=0.05, isotherm increments of 0.05)

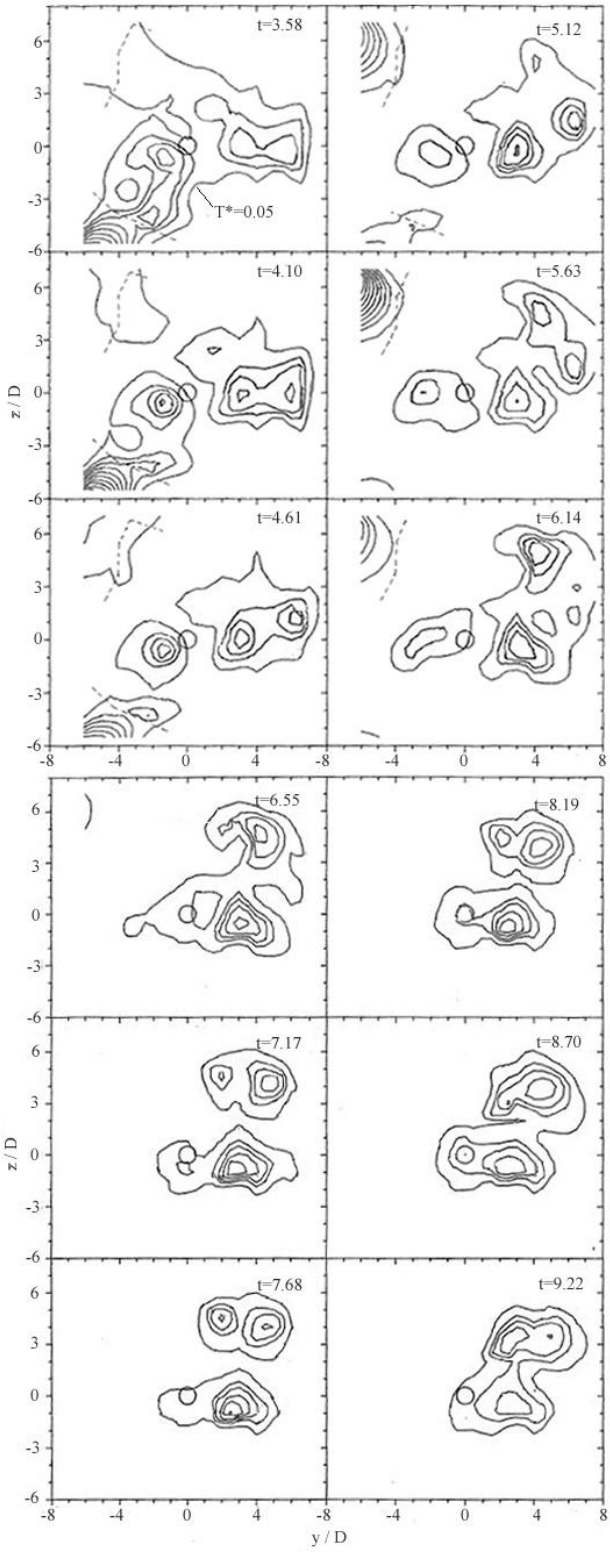

Fig. 4 Instantaneous Contours of Normalized Temperature, $V_J/U=2.3$ (First isotherm at T*=0.05, isotherm increments of 0.05)

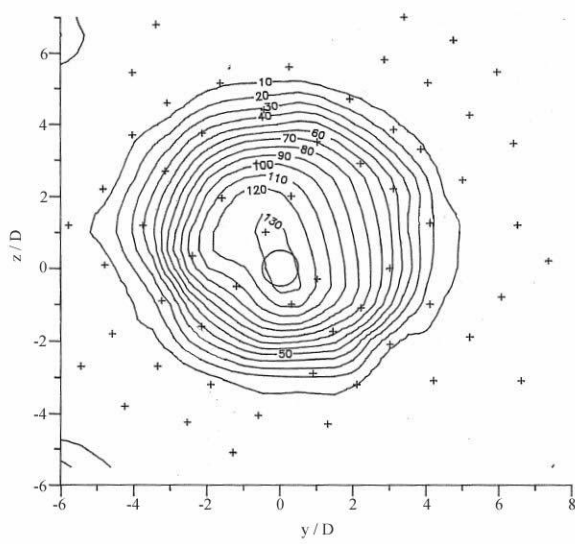

Fig. 5 Contours of Normalized Temperature * 1000, $\tau_s U/D=10^4$, $V_J/U=1.3$

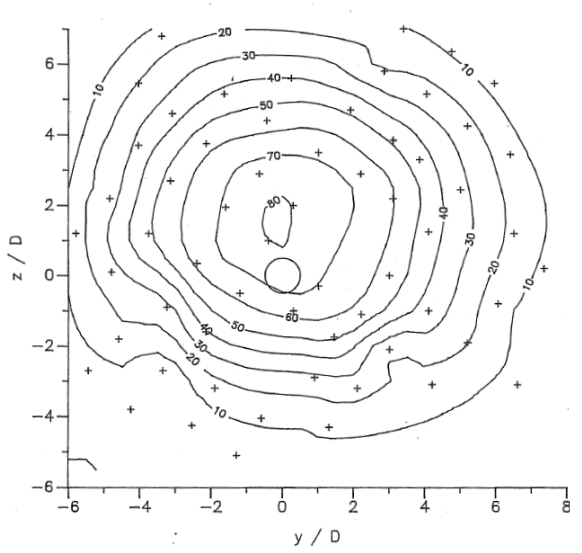

Fig. 6 Contours of Normalized Temperature * 1000, $\tau_s U/D=10^4$, $V_J/U=2.3$

Connections to the T.U. Berlin Research Results

Following the Solfrank (1985) and Moeller (1987) research efforts, the T.U. Berlin investigations: König and Fiedler (1991) and Yoda and Fiedler (1996), clarified that $V_j/U=1.4$ served as an important demarcation between the low velocity ratio behavior and the much more dynamic "high velocity ratio" behavior. The quantitatively different behaviors are well represented in the current results. Specifically, the time averaged isotherms of the $V_j/U=2.3$ condition (see Fig. 6) are distinctly larger in area than those of the $V_j/U=1.3$ condition. Similarly, the instantaneous "temperature islands" of Figs. 3 and 4 show a much larger dispersion for the higher velocity ratio.

The LIF images of the 1996 paper provide instructive physical evidence for the qualitative differences that result for the higher velocity ratio. Specifically, the jet column is seen to be unstable at its farthest extent and the fluid from that region is laterally displaced from the jet axis. The natural consequence – as clearly shown in Fig. 4 – is that the jet fluid is convected back to the plane of the jet exit to create the strongly varying positions of the thermal islands.

The free-stream disturbance level of the MSU ($\tilde{u}/U \lesssim 0.5\%$) and the T.U. Berlin ($\tilde{u}/U = 4\%$) experiments likely sharpen the time-mean velocity ratio effects.

Measures of the Temperature Fields

The instantaneous temperature contours of Figs. 3 and 4 can be understood to represent "temperature islands in the ambient sea." Two properties of these islands can be used to statistically characterize the temperature fields: the peak value (T^*_{max}) and the planar area of the island. For the latter, it was useful to impose an arbitrary level above T*=zero to characterize the perimeter. Values of 0.03 and 0.045 were selected for the $V_j/U=2.3$ and 1.3 cases, respectively. The area of the thermally marked fluid was estimated using triangular patches defined from the irregular array of thermocouples whose positions are shown in Fig 1b (consult Moeller (1987) for the detailed considerations leading to the area values). Dividing by the jet exit area provides A*.

Fig. 7 provides a compact representation of these two quantities by plotting T^*_{max} as a function of A*. Both quantities show a substantial variation and the correlation indicates that the larger is the area, the less is the central fluid heat loss to the surrounding (ambient) fluid. In keeping with other observations, the low velocity ratio case (1.3) exhibits a distinctly stronger correlation between T^*_{max} and A* than does the $V_j/U=2.3$ case.

SUMMARY

A distinctive experimental technique: "capturing instantaneous planes of temperature at the jet exit location" has been used to characterize the upwind directed jet flow field. The temperature data, for this passive contaminant, reveal both the kinematic and the diffusive attributes of this generic flow field. The diffusive effects are substantial. The nominal peak temperatures for the time resolved temperature fields at x=0 were 0.2 for the $V_j/U=2.3$ case and 0.3 for the lower velocity ratio condition: $V_j/U=1.3$.

The time average temperature field shows the expected "quasi-circular" isotherms. A noteworthy aspect of the time average temperature values is the quite significant reductions in the peak temperatures: 0.08 for the larger and 0.13 for the smaller velocity ratios.

The present results are in agreement with those of the T.U. Berlin group regarding the qualitatively different behavior above and below $V_j/U=1.4$. The 1996 Yoda and Fiedler LIF observations of the column instabilities at the higher velocity

ratios can be directly related to the larger lateral displacements of the thermal "islands" at x=0 for V_j/U=2.3 cf 1.3.

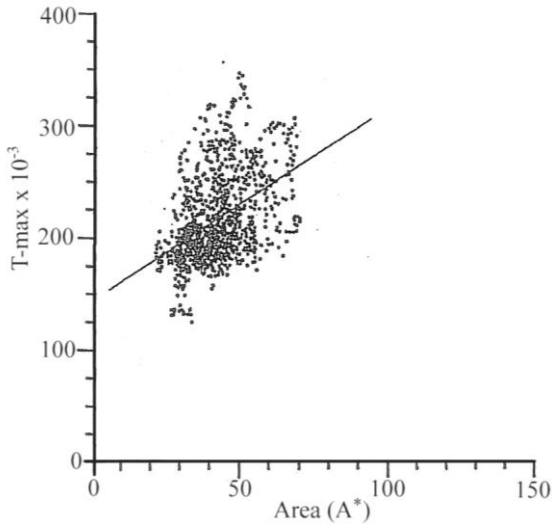

a) V_j/U=1.3

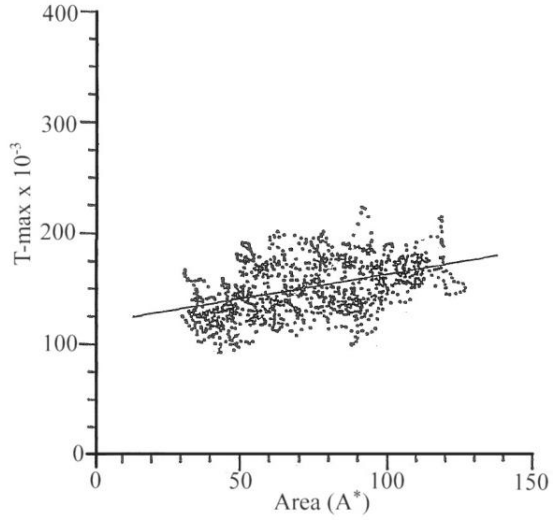

b) V_j/U=2.3

Fig. 7 Individual realizations of T^*_{max} and A* pairings.
Note: solid line shows the correlation axis with the minimum "moment-of-inertia" for the discrete values.

REFERENCES

Arendt, J., Babcock, A.A., Schuster, J.C., "Penetration of a Jet into a Counterflow," *Proc. ASME J. Hydraul. Div.*, **82**:1038/8-/11 (1956).

Bernero, S. and Fiedler, H.E., "Application of particle image velocimetry and proper orthogonal decomposition to the study of a jet in a counterflow," *Exp. in Fluids* [Suppl.] pp. 274-281 (2000).

König, O. and Fiedler, H.E., "The structure of round turbulent jets in counterflow: a flow visualization study," *Advances in turbulence III*, Johansson and Alfredsson, Eds., pp. 61-66 (1991).

Moeller, M, "Thermal and Kinematic Properties of Up-Wind Directed Jets" Diplomarbeit MSU and RWTH (1987).

Morgan, W.D., Brinkworth, B.J., Evans, G.V., "Upstream Penetration of an Enclosed Counterflowing Jet," *Industrial Engineering and Chemistry, Fundamentals*, **15** (1976) pp. 125-127.

Peck, R.E., "Aerodynamics of a Round Jet in a Counterflowing Wind," *AIAA Journal Aircraft*, **18**:1 (1981) pp. 61-62.

Solfrank, P., "Kinematics of Up-Wind Directed Jets," Diplomarbeit at RWTH Aachen, carried out at Michigan State University, Free Shear Flow Laboratory, 1985

Wark, C.E. and Foss, J.F., "Thermal Measurements for Jets in Disturbed and Undisturbed Crosswind Conditions," *AIAA Journal*, **26**:8 (Synoptic) (1988) pp. 901-902.

Yoda, M. and Fiedler, H.E., "The round jet in a uniform counterflow: flow visualization and mean concentration measurements," *Exp. in Fluids*, **21**:427-436 (1996).